

Original citation:

Osman, Ahmed I., Abu-Dahrieh, Jehad K., Cherkasov, Nikolay, Fernández-García, Javier, Walker, David, Walton, Richard I., Rooney, David W. and Rebrov, Evgeny (2018) A highly active and synergistic Pt/Mo₂C/Al₂O₃ catalyst for water-gas shift reaction. *Molecular Catalysis*, 455 . pp. 38-47. doi:10.1016/j.mcat.2018.05.025

Permanent WRAP URL:

<http://wrap.warwick.ac.uk/103633>

Copyright and reuse:

The Warwick Research Archive Portal (WRAP) makes this work by researchers of the University of Warwick available open access under the following conditions. Copyright © and all moral rights to the version of the paper presented here belong to the individual author(s) and/or other copyright owners. To the extent reasonable and practicable the material made available in WRAP has been checked for eligibility before being made available.

Copies of full items can be used for personal research or study, educational, or not-for-profit purposes without prior permission or charge. Provided that the authors, title and full bibliographic details are credited, a hyperlink and/or URL is given for the original metadata page and the content is not changed in any way.

Publisher's statement:

© 2018. This manuscript version is made available under the CC-BY-NC-ND 4.0 license <http://creativecommons.org/licenses/by-nc-nd/4.0/>

A note on versions:

The version presented here may differ from the published version or, version of record, if you wish to cite this item you are advised to consult the publisher's version. Please see the 'permanent WRAP URL' above for details on accessing the published version and note that access may require a subscription.

For more information, please contact the WRAP Team at: wrap@warwick.ac.uk

A highly active and synergistic Pt/Mo₂C/Al₂O₃ catalysts for Water-Gas Shift

Reaction

Ahmed I. Osman ^{a, b*}, Jehad K. Abu-Dahrieh^{a*}, Nikolay Cherkasov^c, Javier Fernandez-Garcia^c,
David Walker^d, Richard I. Walton^e, David W. Rooney^a, Evgeny Rebrov^{c,f}

^a School of Chemistry and Chemical Engineering, Queen's University Belfast, Belfast BT9 5AG,
Northern Ireland, UK

^b Chemistry Department, Faculty of Science-Qena, South Valley University, Qena 83523, Egypt.

^c School of Engineering, University of Warwick, Coventry, CV4 7AL, UK

^d Department of Physics, University of Warwick, Coventry, CV4 7AL, UK

^e Department of Chemistry, University of Warwick, Coventry, CV4 7AL, UK

^f Department of Biotechnology and Chemistry, Tver State Technical University, Russia

ORCID information

Ahmed I. Osman: <http://orcid.org/0000-0003-2788-7839>

Evgeny Rebrov: <http://orcid.org/0000-0001-6056-9520>

Richard Walton: <https://orcid.org/0000-0001-9706-2774>

David W. Rooney: <https://orcid.org/0000-0001-5036-2497>

Nikolay Cherkasov: <https://orcid.org/0000-0001-5979-8713>

Corresponding Author: Ahmed I. Osman, Jehad Abu-Dahrieh

Email: aosmanahmed01@qub.ac.uk, j.abudahrieh@qub.ac.uk

Address: School of Chemistry and Chemical Engineering, Queen's University Belfast, David
Keir Building, Stranmillis Road, Belfast BT9 5AG, Northern Ireland, United Kingdom

Fax: +44 2890 97 4687

Tel.: +44 2890 97 4269

Abstract

Catalysts consisting of Pt and Cu supported on $\text{Mo}_2\text{C}/\eta\text{-Al}_2\text{O}_3$, $\text{Mo}_2\text{C}/\gamma\text{-Al}_2\text{O}_3$ or Mo_2C were prepared and used for the low-temperature water gas shift reaction. The catalysts were characterized by elemental analysis, X-ray diffraction (XRD), temperature-programmed reduction (TPR), X-ray photoelectron spectroscopy (XPS) and scanning electron microscopy (SEM). The catalysts were studied in water gas shift reaction (WGSR) with a reaction mixture containing 11 % CO, 43 % H_2 , 6% CO_2 , 21 % H_2O (real feed composition mixture from the reformer) and balance He, with a reaction temperature range of 180-300 °C at a space velocity (SV) of 125,000 h^{-1} . Catalyst supports ($\eta\text{-Al}_2\text{O}_3$ and $\gamma\text{-Al}_2\text{O}_3$), led to different synergetic effect between the two most active phases of Pt metal and Mo_2C . Pt/ $\text{Mo}_2\text{C}/\eta\text{-Al}_2\text{O}_3$ is a promising catalyst (44% conversion at 180°C) due to the close interaction between Pt and Mo_2C phases on the surface of the catalyst. The 4 Pt- Mo_2C showed the highest activity where the temperature at which 50%

conversion observed was at only 180 °C with SV of 125,000 h⁻¹ and constant stability over 85 hours.

Keywords: Water Gas Shift Reaction; Molybdenum carbide, Platinum, alumina, syngas.

Research highlights

- Molybdenum carbide is the active phase in water gas shift reaction
- The dispersion of Mo₂C during the carburization was enhanced with Pt
- Pt/ Mo₂C catalysts are better than Cu/ Mo₂C modified catalysts in WGSR.
- Using different acidic supports affect the synergetic effect between Pt and Mo₂C.
- Pt/Mo₂C showed higher catalytic activity than that of the commercial CuZnAl catalyst

1. Introduction

Nowadays, great attention is paid toward the water gas shift reaction (WGSR) as it offers a way of producing additional H₂ as well as eliminating harmful CO emissions in a variety of industrial applications to meet the safety and environmental requirements. The rise of bio-oil pyrolysis and subsequent methanol production makes a significant use of research into novel water-gas shift catalysts [1, 2]. The reaction feed for WGSR usually comes from of syngas (a mixture of CO and H₂), generated by various processes such as biomass or coal gasification, methane steam or dry reforming, and methane partial oxidation.

At the industrial scale, the WGSR is carried out in two separate steps, high and low-temperature WGSR, to shift the equilibrium of the exothermic reaction into the desired direction. WGSR is used in preparing gases for fuel cells. High-temperature proton exchange membrane (HT-PEM) fuel cells can tolerate CO concentrations up to 3 vol.% [3], however, for low temperature (LT) fuel cells it is necessary to reduce CO concentration to less than 50 ppm for Pt electrode [4]. The drive for the production of synthetic fuels requires novel compact catalysts with a fast start-up time [5].

Noble metals supported onto reducible oxides represent a large class of novel WGSR catalysts. Choung et al.[6] observed a higher WGSR rate over a bimetallic Pt-Re catalyst supported onto a CeO₂-ZrO₂ mixed metal oxide than the rates calculated by addition of individual rates over monometallic Pt and Re catalysts. The simultaneous addition of both Mo and Pt to WGSR catalysts supported on alumina (or silica) increases CO reaction rate at a temperature around 300 °C [7] which is related to decreasing CO binding energy over PtMo alloys. However, the authors observed a lower TOF over the bimetallic PtMo supported catalysts compared to Pt/CeO₂ catalyst.

Transition metal carbides such as Mo₂C and Co₂C have been established as active and selective catalysts for the WGSR [4, 8, 9]. Gnanamani et al.[10] studied the WGS reaction over alkali-promoted Co₂C catalysts. They found that a Na/Co₂C catalyst showed a CO conversion of 76.3% at 240 °C. The authors suggested that the activity of the cobalt-based catalysts is primarily due to

the carbide phases and the alkali metals (Na and K) promote catalytic activity by keeping cobalt in the reduced state. An active site density in Mo₂C catalysts is 25% greater than that in a commercial Cu/ZnO/Al₂O₃ catalyst. Therefore, the Mo₂C catalysts have a potential to replace the latter in a number of small-scale reactors for WGS [11]. Thin layers of Mo₂C catalysts supported onto a Mo substrate demonstrate catalytic activity in the WGS by 1–2 orders of magnitude higher than that of the commercial Cu/ZnO/Al₂O₃ catalyst [12, 13]. The catalytic activity of a bulk Mo₂C catalyst can further be improved by 4-5 times after the addition of small amounts of Pt [8]. The reaction rate over a Pt/Mo₂C/Al₂O₃ catalyst of 69.2 μmol g_{cat}⁻¹ s⁻¹ was higher as compared to that of 61.8 μmol g_{cat}⁻¹ s⁻¹ over a Cu/Zn/Al₂O₃ catalyst, while the turnover frequency (TOF) over the Pt/Mo₂C/Al₂O₃ catalyst of was reported to be 0.81 s⁻¹ [9].

The highest WGS rate of 284.6 μmol g_{cat}⁻¹ s⁻¹ was observed at 240 °C over a non-supported Pt/Mo₂C catalyst [9]. The exceptionally high activity of the Pt/Mo₂C catalyst prepared by an aqueous wet impregnation method was due to the high density of active sites and the strong interaction between highly dispersed Pt nanoparticles and the Mo₂C support [4]. A high stability of the Pt/Mo₂C catalyst was also reported in the methanol electro-oxidation which has a similar reaction mechanism [14]. It was observed that Pt (i) increased the stability of Mo₂C support due to a strong chemical interaction and (ii) created a synergetic effect between the Pt nanoparticles and the Mo₂C phase.

We have studied precious metal catalysts [15] and molybdenum carbides [12, 16-19] in the medium temperature range. Among the precious metals, a Pt/Mo₂C catalyst has demonstrated the most promising results [5], with the temperature of 50% conversion (T_{50%}) of 180 °C at a space velocity (SV) of 125,000 h⁻¹. Sabnis et al.[8, 20] studied WGS reaction over a Pt/Mo₂C catalyst and proposed a dual-site reaction mechanism. According to this mechanism, the catalytic sites are

located at the interface between the Mo₂C and the Pt nanoparticles. The Mo₂C phase adsorbs and activates water, while the Pt nanoparticle chemisorbs CO [8].

The present work aims at the development of novel Mo₂C-containing catalysts with higher activity and stability in the WGSR, by the addition of the Pt and Cu nanoparticles. Previously we obtained η -Al₂O₃ and γ -Al₂O₃ with different surface and bulk characteristics from Al(NO₃)₃ and AlCl₃ precursors, respectively [21, 22]. Herein, the structure-activity relationship over η -Al₂O₃ and γ -Al₂O₃ supported catalysts with different Mo₂C loadings (33, 50 and 66 wt %) has been studied. While the alumina support allows fast scale-up via screen printing [23], the effect of the catalyst precursor is crucial in heterogeneous catalysis due to its effect on metal dispersion and close interaction between the active sites. Sabnis et al.[8], Wang et al.[9] and Schweitzer et al.[4], used an H₂PtCl₆ precursor to prepare their Pt/Mo₂C catalysts. However, it is well known that the catalysts derived from chlorine-containing precursors could be poisoned by chloride ions adsorbed on the metal surface. For example, the methane total oxidation conversion at 300°C over catalysts prepared from a Cl-containing precursor was much lower as compared to the catalysts prepared from chlorine-free precursors [24, 25].

Herein, we prepared a different range of catalysts using noble (Pt) or transition (Cu) metals loaded on Mo₂C/ η -Al₂O₃, Mo₂C/ γ -Al₂O₃ or Mo₂C for the low-temperature WGSR. Using different acidic supports (η -Al₂O₃ and γ -Al₂O₃) in the catalyst composition, led to different synergetic effect between Pt and Mo₂C. The prepared catalysts were used in WGSR and compared with the

commercial catalyst using a real feed composition mixture from the reformer (11 % CO, 43 % H₂, 6% CO₂, 21 % H₂O).

2. Experimental

2.1 Catalyst preparation

The alumina supports (η -alumina and γ -alumina) were prepared as described in our previous work [21, 26-29] using aluminium nitrate or chloride precursor, after the precipitation by ammonia solution and calcination of the precipitate at 550 °C.

The supported Mo₂C/Al₂O₃ catalysts containing 33, 50 and 66 wt. % Mo₂C were prepared by a wet impregnation of the respective alumina supports with a solution containing ammonium molybdate tetrahydrate precursor ((NH₄)₆Mo₇O₂₄ · 4H₂O; 81-83% as MoO₃, Alfa Aesar). The mixture was sonicated at 80 °C (200 HT Crest ultrasonic bath), at a 45 kHz frequency for 3 h and resulted in a homogeneous paste. Then the mixture was dried at 120 °C overnight and calcined at 500 °C for 4 h under air with a heating rate of 2 °C min⁻¹. After calcination, the sample was crushed, pelletized and sieved to obtain a 225-450 μ m fraction. Finally, the pellets were carburized in a flow of 15 vol.%, CH₄/H₂ (50 ml.min⁻¹) as the temperature was increased from the room temperature to 200 °C at a heating rate of 10 °C.min⁻¹, and then from 200 to 590 °C at a rate of 1 °C.min⁻¹. The temperature was kept at 590 °C for 2 hrs.

The second wet impregnation was used to introduce promoters. In this step, a solution containing Pt(NH₃)₄(OH)₂ or copper (II) acetate monohydrate precursors were used following the procedure described above. The Pt and Cu metal loading in the obtained catalysts were 4 and 20 wt%,

respectively. The samples were designated as X Pt-Y Mo₂C-Z where index X designates the Pt loading in wt%, index Y designates the Mo₂C loading in wt% and index Z designates the type of alumina support E- (η -Al₂O₃) and G- (γ -Al₂O₃).

2.3 Catalyst characterization

The characterisation techniques are described in the supplementary information.

2.4 Catalyst activity measurements

Prior to the catalytic tests, the catalysts were pre-treated in a flow of 15% CH₄/H₂ at a flow rate of 100 mL min⁻¹ at 590 °C for 2 h with a heating rate 10 °C min⁻¹. In these experiments, 100 mg of catalyst (fraction size: 250-425 μ m) was loaded in a fixed-bed reactor made of stainless steel (6 mm OD). The catalyst was placed between two plugs of quartz wool. A mixture of CO, CO₂, H₂, and helium was mixed with the corresponding water amount in order to achieve the desired feed gas composition of 11 vol.% CO, 43 vol.% H₂ and 6 vol.% CO₂, 21 vol.% H₂O, balance - He with a SV of 125,000 h⁻¹. The liquid flow was controlled with a high-performance liquid pump. The products were analyzed by an in-line Perkin Elmer 500 GC equipped with a Hayesep column, thermal conductivity Detector (TCD) and a flame ionization detector (FID).

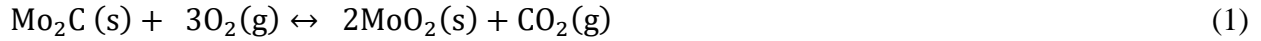
3. Results

3.1. Catalyst characterization

3.1.1. XRD analysis

Figure 1a, shows the XRD patterns of the η -Al₂O₃, Mo₂C, 33 Mo₂C-E, 50 Mo₂C-E and 66 Mo₂C-E catalysts. The XRD patterns of the η -alumina support and a bulk molybdenum carbide catalyst are shown for comparison. The alumina support shows the diffraction peaks corresponding to η -Al₂O₃ (JCD 04-0875). After exposure to air, the Mo₂C phase was oxidized to monoclinic MoO₂ (JCPDS:32-0671) [30]. The appearance of the monoclinic MoO₂ phase can be explained as

follows. After carburization process in the CH₄/H₂ mixture, the molybdenum oxide species were fully converted into β-Mo₂C [9]. Afterwards, β-Mo₂C was converted into MoO₂ by a spontaneous oxidation reaction in the air as seen in Equation 1 and 2 with the final phase composition confirmed by the XRD results [4].



The corresponding diffraction lines of MoO₂, especially those at 2θ= 26.12, 37.11 and 53.58° appeared in both of the studied molybdenum catalysts. The intensity of these lines increased as the molybdenum loading increased from 33 to 66% on η-Al₂O₃ support.

Figure 1b shows the XRD patterns of the γ-Al₂O₃, Mo₂C, 33 Mo₂C-G, 50 Mo₂C-G and 66 Mo₂C-G catalysts. The XRD patterns of the γ-alumina support and a bulk molybdenum carbide catalyst are shown for comparison. The pure alumina support showed the diffraction peaks corresponding to the γ-Al₂O₃ phase (JCDD 10-0425). Once again the bulk Mo-containing catalyst showed monoclinic MoO₂ phase (JCPDS:32-0671) [30]. It is obvious that three of these diffraction lines (2θ= 26.12, 37.11 and 53.58°) appeared in the alumina supported Mo₂C catalysts and these diffraction lines increased in intensity as the molybdenum loading increased from 33 to 66 wt.%. From a previous work [21], the pore volume of η-Al₂O₃ and γ-Al₂O₃ were 0.5 and 0.35 cm³.g⁻¹, respectively, which suggest a higher Mo₂C dispersion on η-Al₂O₃ than that of γ-Al₂O₃.

Table 1 shows the surface area of the pure supports along with the Mo₂C loaded on η-Al₂O₃ or γ-Al₂O₃ support. The BET surface areas of the highest loading Mo₂C on η-Al₂O₃ and γ-Al₂O₃ supports are 100 and 79 m².g⁻¹, respectively. The higher surface area in case of η-Al₂O₃ is due to its higher pore volume than that of γ-Al₂O₃ resulting from a higher Mo₂C dispersion. It is obvious that the surface area decreased with increasing the Mo₂C loading in both η-Al₂O₃ and γ-Al₂O₃ supports by 58 and 95 m².g⁻¹, respectively, while the pore volume decreased by approximately

0.05 cm³.g⁻¹. This decrease in the surface area and pore volume suggested that Mo₂C are filling the pores or deposits on alumina supports.

Table 1: Surface area of the supports along with the metals loaded on Mo₂C/ η -Al₂O₃, Mo₂C/ γ -Al₂O₃ or Mo₂C catalysts.

Catalyst Abbreviation	S _{BET} (m ² .g ⁻¹)	Pore volume (cm ³ .g ⁻¹)
33 Mo ₂ C-E	159	0.27
50 Mo ₂ C-E	130	0.24
66 Mo ₂ C-E	101	0.21
33 Mo ₂ C-G	175	0.18
50 Mo ₂ C-G	131	0.16
66 Mo ₂ C-G	79	0.13
4 Pt-66 Mo ₂ C-E	63	0.10
4 Pt-66 Mo ₂ C-G	37	0.06
20 Cu-66 Mo ₂ C-E	51	0.11
20 Cu-66 Mo ₂ C-G	52	0.07
20 Cu -Mo ₂ C	21	0.03
4 Pt-Mo ₂ C	61	0.10
Mo ₂ C	70	0.11

Figure 2 shows the XRD patterns of Pt or Cu modified Mo₂C or Mo₂C/Al₂O₃ supports. Again, the main three diffraction lines appeared in all of the prepared catalysts. 4 Pt-66 Mo₂C-E and 4 Pt-66 Mo₂C-G catalysts showed two extra diffraction peaks at $2\theta = 39.61$ and 46.42° which corresponding to the reflections (111),(200), respectively, of face-centred cubic (fcc) structure of platinum metal [31, 32] (JCPDS PDF 04-0802). The appearance of platinum diffraction peaks on those two previous supports confirmed a Pt deposition with relatively large particle size over the alumina surface compared with 4 Pt-Mo₂C catalyst which showed no appearance of Pt diffraction peaks; this is may be due to the synergetic effect between Pt and Mo₂C [14, 33]. In copper modified

catalysts, Cu metal diffraction lines (JCPDS 04-0836) appeared at $2\theta = 43.60$ and 50.81° corresponding to (111) and (200), respectively. The 20 Cu-Mo₂C catalyst showed an extra diffraction line at $2\theta = 39.51^\circ$ corresponding to copper oxide phase [34].

Table 1 shows the surface area of the Cu or Pt-modified Mo₂C or Mo₂C/Al₂O₃ supports. Interestingly, the surface area of the pure Mo₂C decreased on loading previously, it was 4 wt% from 70 to 61 m².g⁻¹, and the pore volume remained relatively constant, confirming the synergetic effect between Pt and Mo₂C [14, 33]. The same effect occurred with 20 Cu-Mo₂C as the surface area decreased to 21 m².g⁻¹. Conversely, the surface area of all other catalysts dramatically decreased with loading 4 wt% Pt. For instance, the surface area of 66 Mo₂C-E and 66 Mo₂C-G catalysts were 101 and 79 m².g⁻¹, respectively and decreased by loading Pt to 63 and 37 m².g⁻¹, respectively. The same effect occurred upon loading 20 wt% Cu over these two catalysts as the surface area decreased to 51 and 52 m².g⁻¹, respectively.

3.1.2. H₂-TPR analysis

Figure 3 shows the H₂-TPR profiles of 4 Pt-66 Mo₂C-G, 4 Pt-66 Mo₂C-E, 4 Pt-Mo₂C and 20 Cu-Mo₂C catalysts as each catalyst showed one reduction peak at 20, 9, 88 and 280 °C, respectively. It is well known that using the reducible supports is more active than that of irreducible supports in WGS [4]. It is apparent that all the Pt-containing catalysts reduced much easier than that of Cu containing catalyst. Among the Pt-containing catalysts, 4 Pt-Mo₂C catalyst showed the largest reduction peak which should facilitate the oxidation-reduction cycle and consequently improve the catalytic activity of the catalyst followed by the reduction peak of 4 Pt-

66 Mo₂C-E catalyst. Using the same molybdenum precursor and carburization procedures, pure Mo₂C was prepared by Wang et al.[9] and Schweitzer et al.[4] and H₂-TPR characterization showed a single reduction peak at 250 °C. In our work, loading 4% Pt enhanced the reduction process where the reduction peak shifted to a lower temperature at 88 °C compared to the literature.

3.1.3. SEM-EDX analysis

Figure 4 shows the SEM images of 4 Pt-66 Mo₂C-E, 4 Pt-66 Mo₂C-G, 4 Pt-Mo₂C, and 20 Cu - Mo₂C catalysts. The particles formed clusters in 4 Pt-66 Mo₂C-E, 4 Pt-66 Mo₂C-G, and 20 Cu - Mo₂C catalysts. While the catalyst 4 Pt-Mo₂C catalyst showed good particle size distribution. Moreover, the 4 Pt-Mo₂C catalyst showed smaller particle size than that of the original Mo₂C catalyst as seen in Figure 5.

Table 2 shows the EDX data of Mo₂C, 4 Pt-66 Mo₂C-E, 4 Pt-66 Mo₂C-G, 4 Pt-Mo₂C and 20 Cu - Mo₂C catalysts. EDX showed that 4 Pt-Mo₂C offered the best Pt particle size distribution by showing 4.3 wt% of Pt. While 4 Pt-66 Mo₂C-E and 4 Pt-66 Mo₂C-G catalysts showed Pt content around 5.5 % and this agrees with the SEM images that showed a cluster formation on the surface

of these two catalysts. The copper loading in 20 Cu -Mo₂C was 20 wt%; EDX result showed 18.6% and this is may be due to the poor copper dispersion as shown by SEM images in Figure 4.

Table 2: EDX data of Pure Mo₂C, 4 Pt-66 Mo₂C-E, 4 Pt-66 Mo₂C-G, 4 Pt-Mo₂C and 20 Cu - Mo₂C.

	Pt (wt. %)	Mo (wt. %)	O (wt. %)	Al (wt. %)	Cu (wt. %)
Mo₂C	--	69.5	30.5	--	--
4 Pt-66 Mo₂C-E	5.1	52.0	35.3	7.5	--
4 Pt-66 Mo₂C-G	5.5	48.3	35.9	10.3	--
4 Pt-Mo₂C	4.3	64.6	31.1	--	--
20 Cu -Mo₂C	--	54.4	27.0	--	18.6

3.1.4. Understanding the catalyst structure using XPS analysis

To understand the catalyst structure and molybdenum carbide behaviour of 4 Pt-66 Mo₂C-G, 4 Pt-66 Mo₂C-E, XPS and XRD analyses were utilised. X-ray photoelectron spectra of the partially oxidised samples (left in air for short time) are presented in Figure 6. The Mo peak for the 4 Pt-66 Mo₂C-G sample shows the presence of Mo in three oxidation states; as Mo₂C, MoO₂ and MoO₃ in the molar ratio of 64:11:25, respectively. Figure 6b shows that Pt was present in the metallic form on the catalyst surface. Moreover, there is a small peak of Al which was also observed at the binding energy of around 120 eV and corresponded to the γ -Al₂O₃ support material. Interestingly, the survey spectrum showed Mo to Al mass ratio of 5.8, while the nominal sample composition provided the value of 2.2. A significantly higher relative amount of Mo observed on the surface-specific photoelectron spectroscopy indicates that the Mo compounds efficiently covered the surface of the γ -Al₂O₃ support. The Pt to Mo mass ratio was about 0.057 which agrees with the nominal ratio of 0.060.

Figure 6c shows the Mo 3d peak of the 4 Pt-66 Mo₂C-E catalyst, where three oxidation states of Mo can be observed in the molar ratio of 46:17:37 for Mo₂C, MoO₂ and MoO₃, respectively. The

4 Pt-66 Mo₂C-E sample compared to the 4 Pt-66 Mo₂C-G one shows a lower amount of Mo₂C and an increased MoO₃. In contrast to the 4 Pt-66 Mo₂C-G sample, the 4 Pt-66 Mo₂C-E sample Figure 6d shows the presence of Mo peak close to that for Pt, but no Al. The latter is surprising considering the nominal Al content of 30 wt%. However, considering that XPS is a very surface-specific method, the absence of Al on the spectra can be explained by full coverage of the η -Al₂O₃ support with Mo which is feasible considering high Mo content. The possibility of η -Al₂O₃ coverage is also supported by the very low Pt to Mo mass ratio observed of 0.006 for the 4 Pt-66 Mo₂C-E sample, while the nominal loading was 0.060. Thus, the possible interaction between Pt and Mo₂C which are the two active sites in WGS in the case of 4 Pt-66 Mo₂C-E is shown in Scheme 1. On the other hand, 4 Pt-66 Mo₂C-G showed an interaction between Pt and γ -Al₂O₃ on the surface of the catalyst as shown in Figure 6 b and Scheme 1. Therefore, XPS results revealed that by using different acidic supports (η -Al₂O₃ and γ -Al₂O₃) in the catalyst composition, this led to different interaction because Pt in the catalyst was substantially below the Mo₂C surface as confirmed by the survey spectra and showed in Scheme 1 along with and synergetic effect between the two most active phases of Pt metal and Mo₂C which is greater in the case of 4 Pt-66 Mo₂C-E (η -Al₂O₃) catalyst than that of 4 Pt-66 Mo₂C-G (γ -Al₂O₃). We reported earlier that η -Al₂O₃ and γ -Al₂O₃ catalysts can be prepared from different precursors of aluminium nitrates and chloride, respectively [21]. The produced catalysts showed different surface morphology and acidity with η -Al₂O₃ showed higher acidity and better morphology than that of the γ -Al₂O₃ catalyst. η -Al₂O₃ showed a total acidity and the acid site density of 8.56×10^{20} (sites.g⁻¹) and 3.8×10^{18} (sites.m⁻²), while γ -Al₂O₃ showed values of 6.91×10^{20} (sites.g⁻¹) and 2.5×10^{18} (sites.m⁻²), respectively. Furthermore, η -Al₂O₃ offered a larger pore volume of 0.5 cm³.g⁻¹ compared with that of γ -Al₂O₃

of $0.35 \text{ cm}^3 \cdot \text{g}^{-1}$. The superior morphology and acidity of $\eta\text{-Al}_2\text{O}_3$ offered a better dispersion of Pt with a close interaction with Mo_2C .

Namiki et al.[35] used *in-situ* XPS and DRIFTS techniques to study the mechanism of WGS over Mo_2C catalyst and found that the WGS on the carburised $\text{Mo}_2\text{C}/\text{Al}_2\text{O}_3$ preceded the redox route based on the dissociation of H_2O and CO . Therefore, a good WGS catalyst indicates a facile reduction/oxidation cycle between the two phases of Mo_2C and MoO_x under reaction conditions, thus we investigated the nature of the re-oxidation of Mo_2C phase. The *in-situ* XRD study shown in Figure S1 (supplementary) demonstrate that the carburized catalyst then left in air for a short time (4 Pt-66 Mo_2C -E, reduced) has Pt, Mo_2C and MoO_3 phases. Even gentle heating

to 100 °C in the air (4 Pt-66 Mo₂C-E, fresh) results in a significant decrease in the relative intensity of the Mo₂C reflections and increase in MoO₂ indicating the quick oxidation of the carbide.

4. Catalytic activity

It was reported that Mo₂C showed higher catalytic activity than that of commercial catalyst for WGSR [4]. Herein, we used different supports with copper or platinum loadings as described in Table 1. Figure 7 a shows the catalytic activity profiles for WGSR over Mo₂C, 33 Mo₂C-E, 50 Mo₂C-E and 66 Mo₂C-E catalyst with different Mo₂C loadings over the temperature range 180-300 °C. The conversion increases with increasing either the reaction temperature or the Mo₂C loading, which can be explained as Mo₂C is the only active site for the WGSR and is responsible for the dissociation of water to react with the CO species. The same trend is noticed in the 33 Mo₂C-G, 50 Mo₂C-G, 66 Mo₂C-G and Mo₂C catalysts as shown in Figure 7b but with less catalytic activity at the same Mo₂C loading and different support. For instance, the conversion at 300 °C for 66 Mo₂C-E and 66 Mo₂C-G are 27.17 and 24.1, respectively. The higher activity in the presence of η-Al₂O₃ support can be attributed to the synergetic effect between Pt and Mo₂C as shown from the XPS results in Figure 6 and Scheme 1 along with the higher pore volume of 0.5 for η-Al₂O₃ and 0.35 for γ-Al₂O₃. Although Mo₂C, 66 Mo₂C-E and 66 Mo₂C-G showed the highest catalytic activity in the previous series of catalysts, those catalysts still require further promotion to achieve better catalytic activity and stability during the WGSR. Thus, 4 wt.% Pt and 20 wt.% Cu metals were added to that catalyst where the final prepared catalysts designated as 4 Pt-Mo₂C, 4 Pt-66 Mo₂C-E, 4 Pt-66 Mo₂C-G, 20 Cu-Mo₂C, 20 Cu-66 Mo₂C-E and 20 Cu-66 Mo₂C-G.

Figure 8 shows the catalytic activity for WGSR over different catalysts of 4 Pt-Mo₂C, 4 Pt-66 Mo₂C-E, Mo₂C, 4 Pt-66 Mo₂C-G, 20 Cu -Mo₂C, 20 Cu-66 Mo₂C-E, 20 Cu-66 Mo₂C-G along with the commercial CuZnAl catalysts. In all catalysts, the CO conversion increased with increasing the reaction temperature. All the copper catalysts loaded Mo₂C or Mo₂C-alumina support exhibit low activity at reaction temperatures below 250 °C and have lower conversion than the Pt-based catalysts. For instance, at a reaction temperature of 300 °C, 20 Cu -Mo₂C and 4 Pt-Mo₂C have catalytic conversions of 58 and 81.9 %, respectively. Such differences can be attributed to the active site in metal/Mo₂C catalysts is bi-functional for WGSR as proved by Sabnis et al.[20].

Moreover, the reducibility of the catalyst can play a big role in the catalytic activity, as confirmed by the TPR results, where the reduction temperature for 20 Cu -Mo₂C was 280 °C whereas for 4 Pt-Mo₂C is 88 °C.

For the catalyst to meet the commercialization requirements, it should offer good stability behaviour during the operating conditions. Figure 9 shows a comparison of the stability of Mo₂C, 4 Pt-66 Mo₂C-E and 4 Pt-Mo₂C at a reaction temperature of 250°C for 85 h. The catalytic activity of 4 Pt-66 Mo₂C-E and 4 Pt-Mo₂C is similar at time zero on stream but with time on stream, the CO conversion over 4 Pt-66 Mo₂C-E decreased from 68 to 43% after 30 h then stabilised for the next 55 h, while 4 Pt-Mo₂C was stable over the reaction time which is in agreement with the results of Yan et al.[14].

Compared with the literature, our results show 4-5 times higher activity with the T_{50%} for Pt-Mo₂C was 180°C which is lower than in previous research work performed over the Pt/CeO₂

catalyst, which showed the $T_{50\%}$ value of 400°C [36]. On the addition of Pt, the stability experiments showed no decrease in the catalyst activity over 85 hours at 250 °C.

5. Conclusion

Herein different Pt and Cu based catalysts at different supports (Mo₂C, 4 Pt-66 Mo₂C-E and 4 Pt-66 Mo₂C-G) were studied for low-temperature water gas shift reaction. The prepared catalysts were used in WGSR and compared with the commercial catalyst using a real feed composition mixture from the reformer (11 % CO, 43 % H₂, 6% CO₂, 21 % H₂O). It was found that the 4 Pt-Mo₂C catalyst has the highest activity and the most stable catalyst over 85 hours at 250 °C. XPS

results revealed that by using different acidic supports (η -Al₂O₃ and γ -Al₂O₃) led to different interaction and synergetic effect between the two most active phases of Pt metal and Mo₂C.

Acknowledgement

The financial support from the FP7-NMP project BIOGO (grant: 604296) is kindly acknowledged.

Conflict of Interest Statement: The authors declare no conflict of interest.

6. References

- [1] C. Ratnasamy, J.P. Wagner, *Catalysis Reviews*, 51 (2009) 325-440.
- [2] R. Burch, *Physical Chemistry Chemical Physics*, 8 (2006) 5483-5500.
- [3] P. Sangeetha, K. Shanthi, K.S.R. Rao, B. Viswanathan, P. Selvam, *Applied Catalysis A: General*, 353 (2009) 160-165.
- [4] N.M. Schweitzer, J.A. Schaidle, O.K. Ezekoye, X. Pan, S. Linic, L.T. Thompson, *Journal of the American Chemical Society*, 133 (2011) 2378-2381.
- [5] C. Wheeler, A. Jhalani, E.J. Klein, S. Tummala, L.D. Schmidt, *Journal of Catalysis*, 223 (2004) 191-199.
- [6] S.Y. Choung, M. Ferrandon, T. Krause, *Catalysis Today*, 99 (2005) 257-262.
- [7] W.D. Williams, L. Bollmann, J.T. Miller, W.N. Delgass, F.H. Ribeiro, *Applied Catalysis B: Environmental*, 125 (2012) 206-214.
- [8] K.D. Sabnis, Y. Cui, M.C. Akatay, M. Shekhar, W.-S. Lee, J.T. Miller, W.N. Delgass, F.H. Ribeiro, *Journal of Catalysis*, 331 (2015) 162-171.
- [9] G. Wang, J.A. Schaidle, M.B. Katz, Y. Li, X. Pan, L.T. Thompson, *Journal of Catalysis*, 304 (2013) 92-99.
- [10] M.K. Gnanamani, G. Jacobs, W.D. Shafer, D.E. Sparks, S. Hopps, G.A. Thomas, B.H. Davis, *Topics in Catalysis*, 57 (2014) 612-618.
- [11] D.J. Moon, J.W. Ryu, *Catalysis Letters*, 92 (2004) 17-24.
- [12] A.R. Dubrovskii, S.A. Kuznetsov, E.V. Rebrov, J.C. Schouten, *Russian Journal of General Chemistry*, 82 (2012) 2070-2078.
- [13] A.R. Dubrovskii, S.A. Kuznetsov, E.V. Rebrov, J.C. Schouten, *Russian Journal of Applied Chemistry*, 87 (2014) 601-607.
- [14] Z. Yan, H. Wang, M. Zhang, Z. Jiang, T. Jiang, J. Xie, *Electrochimica Acta*, 95 (2013) 218-224.
- [15] E.V. Rebrov, A. Berenguer-Murcia, B.F.G. Johnson, J.C. Schouten, *Catalysis Today*, 138 (2008) 210-215.
- [16] E.V. Rebrov, S.A. Kuznetsov, M.H.J.M. de Croon, J.C. Schouten, *Catalysis Today*, 125 (2007) 88-96.
- [17] S.A. Kuznetsov, A.R. Dubrovskiy, E.V. Rebrov, J.C. Schouten, *Zeitschrift für Naturforschung A*, 62 (2007) 647-654.
- [18] A.R. Dubrovskii, S.A. Kuznetsov, E.V. Rebrov, J.C. Schouten, *Kinetics and Catalysis*, 49 (2008) 594-598.
- [19] A.R. Dubrovskiy, E.V. Rebrov, S.A. Kuznetsov, J.C. Schouten, *Catalysis Today*, 147, Supplement (2009) S198-S203.
- [20] K. Sabnis, M. Shekhar, J. Lu, M.C. Akatay, J. Elam, J.T. Miller, W.N. Delgass, F.H. Ribeiro, in: *AIChE 2012 - 2012 AIChE Annual Meeting, Conference Proceedings*, 2012.
- [21] A.I. Osman, J.K. Abu-Dahrieh, D.W. Rooney, S.A. Halawy, M.A. Mohamed, A. Abdelkader, *Applied Catalysis B: Environmental*, 127 (2012) 307-315.
- [22] A.I. Osman, J.K. Abu-Dahrieh, *Catalysis Letters*, 148 (2018) 1236-1245.
- [23] H. Pennemann, M. Dobra, M. Wichert, G. Kolb, *Chemical Engineering & Technology*, 36 (2013) 1033-1041.
- [24] A.I. Osman, J.K. Abu-Dahrieh, F. Laffir, T. Curtin, J.M. Thompson, D.W. Rooney, *Applied Catalysis B: Environmental*, 187 (2016) 408-418.
- [25] A.I. Osman, J.K. Abu-Dahrieh, M. McLaren, F. Laffir, D.W. Rooney, *ChemistrySelect*, 3 (2018) 1545-1550.
- [26] A.I. Osman, J. Meudal, F. Laffir, J. Thompson, D. Rooney, *Applied Catalysis B: Environmental*, 212 (2017) 68-79.
- [27] A.I. Osman, J.K. Abu-Dahrieh, D.W. Rooney, J. Thompson, S.A. Halawy, M.A. Mohamed, *Journal of Chemical Technology & Biotechnology*, 92 (2017) 2952-2962.
- [28] A.I. Osman, J.K. Abu-Dahrieh, M. McLaren, F. Laffir, P. Nockemann, D. Rooney, *Nature Scientific Reports*, 7 (2017) 3593.
- [29] A.I. Osman, J.K. Abu-Dahrieh, A. Abdelkader, N.M. Hassan, F. Laffir, M. McLaren, D. Rooney, *The Journal of Physical Chemistry C*, 121 (2017) 25018-25032.
- [30] S. Yoon, A. Manthiram, *Journal of Materials Chemistry*, 21 (2011) 4082-4085.
- [31] T. Hyde, *Platin Met Rev*, 52 (2008) 129-130.

- [32] M.A. Shah, *Scientia Iranica*, 19 (2012) 964-966.
- [33] K. Zhang, W. Yang, C. Ma, Y. Wang, C.W. Sun, Y.J. Chen, P. Duchesne, J.G. Zhou, J. Wang, Y.F. Hu, M.N. Banis, P. Zhang, F. Li, J.Q. Li, L.Q. Chen, *Npg Asia Materials*, 7 (2015) 1-10.
- [34] S. Elzey, J. Baltrusaitis, S. Bian, V.H. Grassian, *Journal of Materials Chemistry*, 21 (2011) 3162-3169.
- [35] T. Namiki, S. Yamashita, H. Tominaga, M. Nagai, *Applied Catalysis A: General*, 398 (2011) 155-160.
- [36] C. Wheeler, A. Jhalani, E.J. Klein, S. Tummala, *Journal of catalysis*, (2004).